DETERMINATION OF PLAGIOCLASE WITH THE FOUR-AXIS UNIVERSAL STAGE

FRANCIS J. TURNER, *University of California, Berkeley, California.*

ABSTRACT

The paper outlines a procedure for measuring optical and crystallographic directions in twinned plagioclase with a four-axis universal stage. Identification of twinning laws and determination of anorthite content are discussed, with special reference to ambiguous cases at the sodic and calcic ends of the plagioclase series. The standard data of Duparc and Reinhard and Nikitin, regarding variation in the crystallographic orientation of the indicatrix with composition (conventionally shown by migration curves in stereographic projection), are presented as a series of curves based on rectangular coordinates. Special cases where one of the directions X, Y or Z coincides with, or is normal to, a twinning axis are reviewed. Finally, attention is drawn to a general tendency, commented upon by a number of writers, for discrepancy between points plotted from data measured on a universal stage, and the standard curves.

INTRODUCTION

The only comprehensive account of universal-stage technique in English—that of R. C. Emmons (1943)—is written for users of the Emmons stage (Bausch and Lomb) with five rotation axes. Some American and British laboratories are equipped only with four-axis stages, such as that formerly manufactured by the firm of Leitz; and moreover there are petrographers (of whom the writer is one) who prefer the four-axis stage for most measurements, and particularly for petrofabric analysis. This paper is written for those who use a four-axis stage for optical determination of feldspars.* It is assumed that the reader is familiar with such elementary procedures as location of X Y and Z, and measurement of optic axial angle.

The objects of the paper are:

(1) To stage concisely by means of illustrative examples the procedure of W. Nikitin (1936) for determining composition of plagioclase.

(2) To make available for routine laboratory use the optical data given by Nikitin in his comprehensive colored plate (Nikitin, 1936, pl. vii). (This may then be preserved from the inevitable damage resulting from constant handling.)

(3) To state, with appropriate diagrams, additional crystallographic data necessary for unambiguous identification of the twinning axes.

(4) To discuss the numerous cases where the measured data may lead to ambiguous determinations of twinning law or of anorthite content.

(5) To draw attention to various anomalies discussed in detail in the

* Since only the innermost rotation axis and the N–S and E–W tilting axes of the stage are used, the procedures described in this paper could equally well be carried out with a three-axis stage.

important but hitherto neglected paper of C. T. Barber (1936*a*).

Use of symbols for crystallographic and optical planes and directions throughout this paper is illustrated by the following examples:

CP_{1-2} = composition plane common to subindividuals (1) and (2) in a twinned grain.

$\perp CP_{1-2}$ = pole of CP_{1-2}, or normal to CP_{1-2}.

Cl_1 = cleavage plane in subindividual (1).

$\perp Cl_1$ = pole of Cl_1, or normal to Cl_1.

$^2CP_1$ = second set of twin lamellae (transverse to CP_{1-2}) cutting across subindividual (1).

$\perp(001)$ = pole of (001), or normal to (001).

[100], [010], [001] = *a*, *b* and *c* crystal axes, respectively.

$\frac{\perp[001]}{(010)}$ = normal to the *c* axis within the plane (010).

A_{2-3} = twinning axis for two twinned subindividuals (2) and (3).

a_1 = optic axis in subindividual (1).

Measurement Procedure

If, as is usually the case, the crystal to be measured shows obvious twinning, it is first roughly sketched, and the various subindividuals appropriately numbered. For each subindividual, the three principal directions X, Y and Z are located with reference to the plane of the microsection. This is done by bringing at least two of these directions in turn to coincide with the E–W axis of the stage, by alternate rotation to extinction on the innermost vertical axis and tilting to extinction on the N–S axis (for different degrees of tilt on E–W).

Example:—In subindividual (1), one of the principal optical directions is brought to coincide with E-W when the reading on the scale of the innermost vertical rotation axis is 79°, and the tilt on N–S is 30° downward to the observer's left. The direction parallel to E-W is identified (by rotating the whole stage through 45° and testing with a gypsum plate) as Z. The result is recorded thus:

$$Z_1 \quad 79 \leftarrow 30$$

A corresponding record for readings when Y of the same subindividual is brought parallel to E–W, is

$$Y_1 \quad 355 \rightarrow 9$$

X_1 is located later by plotting on a projection.

In each subindividual, cleavage and composition planes are sought and brought into coincidence with the plane which contains the E–W tilting axis and the main vertical axis of the microscope. This involves setting the N–S axis at zero, rotating the section on the innermost vertical axis till the trace of the plane to be measured coincides with E–W, and then tilting on E–W to give the sharpest definition possible. Great accuracy

of measurement is difficult to attain, but is unnecessary in cases where twin axes are used in determining composition.

Example:—Composition planes for all three pairs of subindividuals (1), (2) and (3), coincide with the vertical plane parallel to E–W, when the scale reading for the innermost rotation axis is 18°, and the tilt on E–W is 22° toward the observer. The record is

$$CP_{1-2-3} \qquad 18 - 22 \downarrow$$

Fine transverse twin lamellae and accompanying cleavage locally developed in subindividual (3) are similarly brought parallel to the E–W vertical plane when the scale for the innermost vertical rotation axis reads 104° and the tilt on E–W is 16° away from the observer. This is recorded thus,

$$^2CP_3(= {}^2Cl_3) \qquad 104 - 16 \uparrow$$

The complete data for a phenocryst of plagioclase showing three sets of subindividuals large enough to be measured, and local additional fine transverse lamellae in one of these, were recorded thus (cf. Fig. 1):

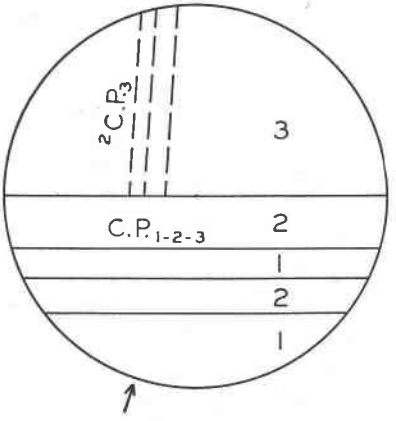

FIG. 1. Plagioclase twinned on ablite (1–2) and Carlsbad (2–3) laws, with second set of twinning and cleavage showing in one subindividual (3).

Y_1	$355 \rightarrow 9$, $a_1 20 \uparrow$
Z_1	$79 \leftarrow 30$
Y_2	$44 \leftarrow 9$, $a_2 41 \uparrow$
Z_2	$316 \rightarrow 10$
X_3	$11 \rightarrow 9$
Y_3	$290 \leftarrow 42$
CP_{1-2-3}	$18 - 22 \downarrow$
$^2CP_3(= {}^2Cl_3)$	$104 - 16 \uparrow$

The expression "a_1 20" after Y_1, indicates the position of an optic axis which is brought to coincide with the vertical axis of the microscope by tilting on E–W through 20° away from the observer, when Y_1 has first been brought parallel to E–W.

Projection Procedure

Points of emergence of the measured directions Y_1, Z_1, Y_2, Z_2, X_3, Y_3, and poles of the measured composition and cleavage planes are now plotted on a suitable projection. Either a stereographic net (Wulff net) or an equal-area net (Schmidt net) will serve for this purpose. The writer somewhat prefers the latter, since the linear scale for a given angular distance (e.g. 10°) is more nearly uniform in a Schmidt net, and rapid plotting in the central part of the projection is thereby somewhat facilitated. In any case the numbering of the divisions on the circumference of the net must correspond with that of the scale for the innermost rotation axis of the stage—usually a clockwise sequence from 0° to 360°, with the zero point at the south pole. The net is covered with transparent paper which can be rotated freely about the center of the net. In the examples given below the *lower* hemisphere is projected, since this conforms to the standard procedure of petrofabric analysis, and at the same time simplifies the process of plotting.

Examples: (1) To plot X_1, Y_1 and Z_1, given

Y_1 $\quad 355 \rightarrow 9$, a_1 $20 \uparrow$;
Z_1 $\quad 79 \leftarrow 30$.

Rotate the tracing sheet until the marginal index arrow (arbitrarily drawn) stands at 79° on the net. On the E–W diameter of the net plot Z_1, 30° in from the E end. Rotate the sheet till the index stands at 355° on the net, and plot Y_1, 9° in from the W end of the E–W diameter of the net. Z_1 should now lie on or close to the great circle at 90° from Y_1. On this circle plot X_1, 90° from Z_1. The axial point A_1 may also be plotted 20° upward from the E–W diameter on the great circle containing X_1 and Z_1. Note that on projections of the lower hemisphere, the direction in which any point is plotted is the same as that of the arrow in the corresponding recorded data.

(2) To plot CP_{1-2-3} $18-22 \downarrow$: Rotate the tracing sheet till the index stands at 18° on the net, and plot the pole of CP_{1-2-3} (i.e. $\perp CP_{1-2-3}$) on the N–S diameter of the net, 22° down from the N end. In the case of feldspars it is convenient also to plot the trace of the main composition plane upon the projection, i.e., to draw the great circle at 90° from the pole of the plane in question (full arc in Fig. 2).

Determination of Twinning Law and Composition of Feldspar from the Plotted Data

The completed projection shows X, Y and Z for each subindividual, together with poles of all measured composition and cleavage planes, projected upon the plane of the thin section. It is possible now to estimate the composition of the feldspar by measuring on the projection the mean angles between each of X, Y and Z, and the poles of observed composition and cleavage planes, using the curves of Fig. 5. Since direct measurement of these crystallographic planes may be attended by considerable error, the writer prefers, wherever possible, to use twinning

axes as axes of reference with which to compare the relative positions of X, Y and Z in each subindividual (cf. Nikitin, 1936, p. 103). To do this it is first necessary to identify the twinning law in question before referring to the curves of Figs. 5 to 7. The types of twinning commonly encountered in feldspars are summarized below:

Type	*Name*	*Composition plane*	*Twinning axis*	*Comments*
Normal	Albite	(010)	$\perp(010)$	Usually multiple
Normal	Manebach	(001)	$\perp(001)$	Usually simple
Normal	Baveno	(021) or $(0\bar{2}1)$	$\perp(021)$ or $\perp(0\bar{2}1)$	Usually simple; rare in plagioclase
Parallel	Carlsbad	(010)	[001]	Simple
Parallel	Ala B	(010)	[100]	Usually multiple
Complex	Albite-Carlsbad	(010)	$\frac{\perp[001]}{(010)}$	Usually multiple
Complex	Albite-Ala	(010)	$\frac{\perp[100]}{(010)}$	Usually multiple
Parallel	Acline	(001)	[010]	Usually multiple
Parallel	Ala A	(001)	[100]	Usually multiple
Complex	Manebach-Acline	(001)	$\frac{\perp[010]}{(001)}$	Optically indistinguishable from Ala A
Complex	Manebach-Ala	(001)	$\frac{\perp[100]}{(001)}$	Optically indistinguishable from Acline
Parallel	Pericline	Rhombic Section	[010]	Optically indistinguishable from Acline in plagioclase of medium composition

The following routine procedure is recommended for determining first the twinning law by which two subindividuals are related, and second their mean composition.

(1) If the directions X_1, X_2, etc. have been accurately located in subindividuals (1) and (2), and if the composition of the measured subindividuals is uniform, the point of emergence of the twinning axis A_{1-2} upon the projection is the point of intersection of the three great circles respectively containing X_1 and X_2, Y_1 and Y_2, Z_1 and Z_2. Usually these arcs do not intersect at a point, but form the boundaries of a triangle of error, the center of which gives the approximate location of the twinning axis. Even when this triangle is fairly large—especially when the angle of intersection of two great circles is small—the results need not be discarded, since exact location of the twinning axis is not essential for approximate determination of composition. Two general cases may at once be distinguished:

(a) The twinning axis coincides with, or approximates to, the plotted pole of the composition plane (as the case of A_{1-2}, Fig. 2). The twin is of the normal type, and the twinning axis (excluding the remote possibility of a Baveno twin) is either $\perp(010)$ or $\perp(001)$.

(b) The twinning axis lies within or close to the arc representing the projection of the composition plane (as in the case of A_{1-3} and A_{2-3}, Fig. 2). The twin is then of either the parallel or the complex type.

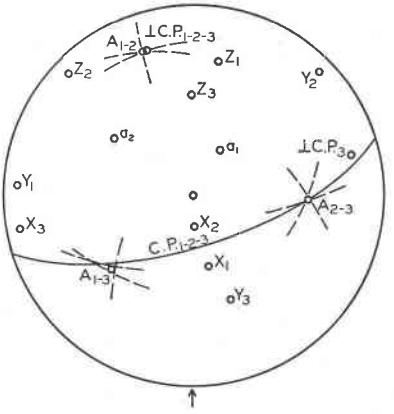

FIG. 2. Equal-area projection (lower hemisphere) of optical and crystallographic data for plagioclase crystal of Fig. (1), twinned on albite and Carlsbad laws.

(2) In either case the mean values are now obtained for the three angles between the twinning axis and each of X, Y and Z, respectively. Rotate the sheet until X_1 and X_2 lie on a great circle of the projection net, and measure the angular distance between them across the arc within which the twinning axis emerges. Half this measured angle $X_1 \wedge X_2$ is the mean value for $X \wedge A_{1-2}$. Similarly measure and halve the appropriate angles $Y_1 \wedge Y_2$ and $Z_1 \wedge Z_2$.

(3) For parallel and complex twins, now measure the angle between the twinning axis and the pole of the second set of twin lamellae or cleavage planes crossing one or other of the two subindividuals in question (e.g. $\perp^2CP_3$ or $\perp^2Cl_3$). The angle so obtained can be used to identify the twinning axis. Since neither of the measured points is accurately located on the projection, the angle between them cannot in some cases be determined with greater accuracy than $\pm 5°$. Except in the case of very sodic or very calcic plagioclase where the transverse lamellae are of the pericline type, this error is immaterial in identifying the twin axis.

(4) The following illustration shows how the data obtained above may be utilized in the final determination. The angles measured on the projection, Fig. 2, are:

Twin 1–2. Normal twin

$A_{1-2} \wedge X$	81°
$\wedge Y$	64°
$\wedge Z$	27°

Twin 2–3. Parallel or complex twin

$A_{2-3} \wedge X$	51°
$\wedge Y$	51°
$\wedge Z$	62°
$A_{2-3} \wedge \perp^2CP_3$	28°±

Twin 1–3. Parallel or complex twin

$A_{1-3} \wedge X$	41°
$\wedge Y$	51°
$\wedge Z$	$80\frac{1}{2}$°
$A_{1-3} \wedge \perp^2CP_3$	63°±

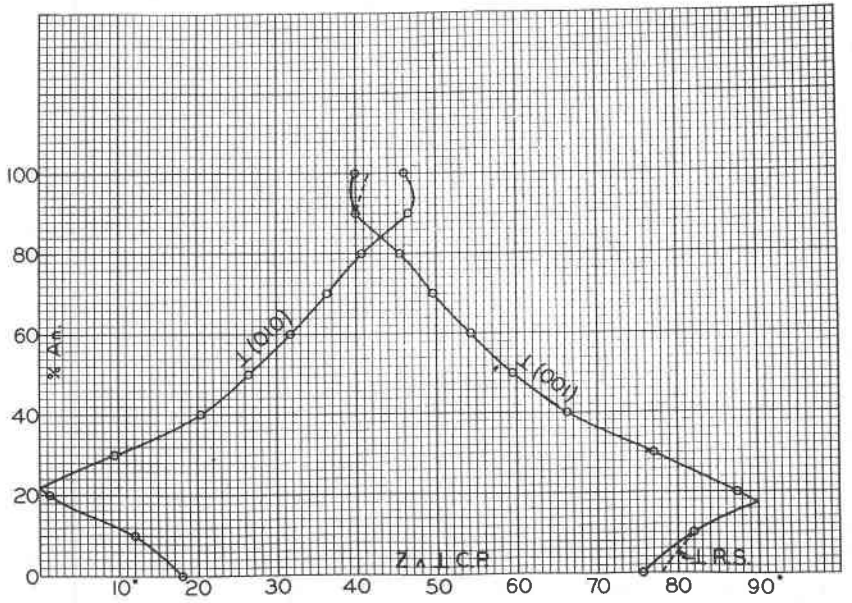

FIG. 3. Relation of angle between Z and the normal to the composition plane (Z∧⊥C.P.), and anorthite content in plagioclase. Broken curve refers to normal to rhombic section.

(a) *Twin 1–2.* Since this is a normal twin, reference is made to Fig. 5. The respective angles between the twinning axis and each of X and Y are plotted one against the other to give a point P close to the curve for ⊥(010). This establishes the twinning axis as ⊥(010) and composition plane as (010) (albite law). The composition is given as An_{49} by the point where the normal drawn from P intersects the curve. (The numbers 0–10 on this and all other curves of Figs. 5–7 correspond to anorthite percentages 0–100.)

(b) *Twin 2–3.* It has just been shown that the common composition plane for all three measured subindividuals is (010). If this had not previously been done it would be necessary to measure separately the angle $Z/\backslash \perp CP_{2-3}$ (29°), which identifies the composition plane CP_{2-3} as (010) (cf. Figs. 3 or 4). To determine the twinning axis* plot on Fig. 4 the angles $A_{2-3}/\backslash \perp^2 CP_3 = 28° \pm$, and $Z/\backslash \perp CP_{2-3} = 29°$; then the twin-

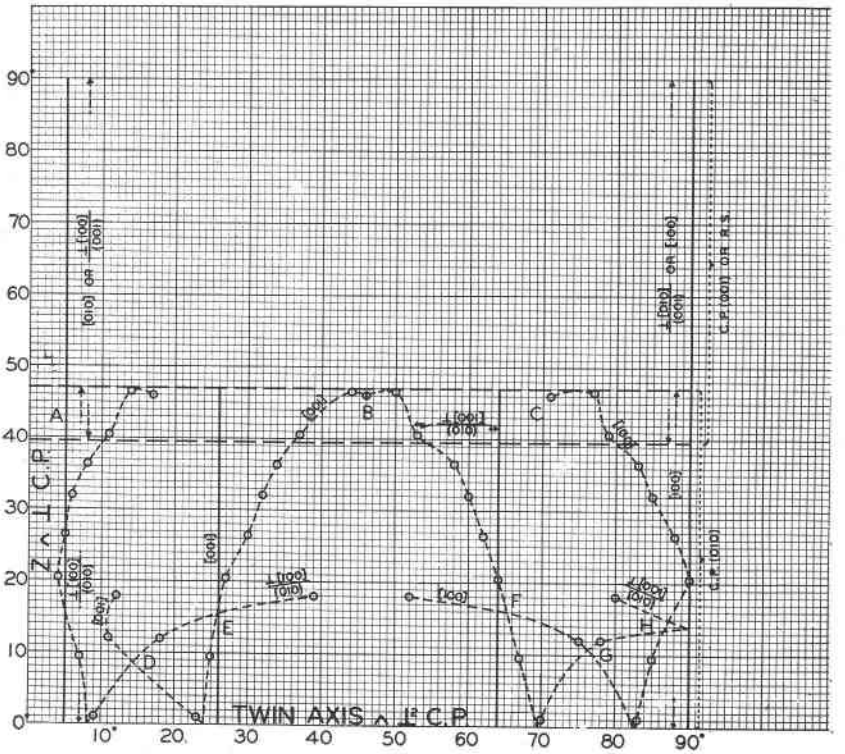

FIG. 4. Angle between twinning axis and normal to second composition plane or cleavage plane, plotted against $Z/\backslash \perp$C.P. Broken curve applies where the second composition plane is the rhombic section.

ning axis must be [001] (Carlsbad law). Now referring to the corresponding curve of Fig. 6 plot the angles $A_{2-3}/\backslash X$ and $A_{2-3}/\backslash Y$, to give *P* which indicates a mean composition An_{47}.

* Nikitin (1936, p. 102), Emmons (1943, p. 156) and others identify the twinning axis of a parallel or complex twin merely by noting to which of the standard migration curves (equivalent to those of Figs. 6 and 7 in this paper) the plotted point representing the positions of X, Y and Z lies closest. The writer has found this unsatisfactory since the curves in question often lie close together, and the plotted point may be as much as 5° or 10° from the curve to which it actually belongs. It is therefore recommended that as far as possible the twinning axis should be identified before the optical data are plotted on Figs. 6 and 7.

(c) *Twin 1–3.* From the above, it follows that subindividuals (1) and (3) must be related by twinning on the Carlsbad-albite law with $\perp[001]/(010)$ as twinning axis. This is confirmed (Fig. 4) by the angle $A_{1-3} \wedge \perp^2 CP_3 = 63° \pm$. Plotting the corresponding X and Y angles on Fig. 7 gives a point *P* indicating a composition An_{45}.

A discrepancy between the values for composition as determined in

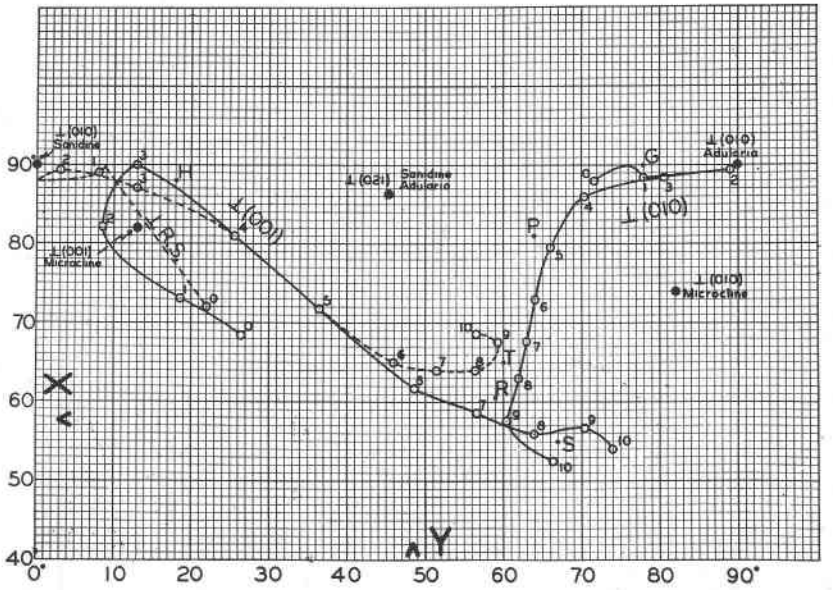

FIG. 5. Angles between X and Y and normals to composition planes in plagioclase. Numbers 0–10 on each curve indicate anorthite contents 0–100%.

different pairs of subindividuals belonging to a single crystal (in the above case An_{49}, An_{47}, An_{45}) is by no means uncommon. It shows that even with a universal stage the An content of plagioclase cannot be determined more closely than $\pm 3\%$.

The above case has been described fully so that the reader may check the method by carrying out each step in turn. Contrary to widely prevalent belief the procedure is neither complex nor unduly lengthy. Optical measurements, projection of the measured data, and subsequent identification of twin laws and determination of composition in this particular case took about 30 minutes. Ten to fifteen minutes should suffice for a crystal in which only two subindividuals are completely measured; while a determination based on measurement of X, Y and Z and one set of cleavages in an untwinned grain (using Fig. 5) takes less than ten minutes.

Ambiguous Cases

If observations are confined to two subindividuals, a number of cases involving some degree of ambiguity commonly arise. Most of these may be solved satisfactorily if additional data are obtained from other subindividuals of the same crystal.

(a) *Ambiguous cases with normal twinning*

(1) In Fig. 5 (cf. also Figs. 3 and 4), identification of the twinning axis of normal twins for the range An_{70} to An_{100} is usually uncertain. Direct measurement of the second (transverse) set of cleavage planes or twin lamellae in one of the principal subindividuals, and determination of the angles between X and Y respectively and the pole of this second plane usually leads to an unambiguous solution.

Example:

$$A_{1-2} \wedge X = 60\tfrac{1}{2}^\circ$$
$$\wedge Y = 59^\circ$$

The corresponding point *R* in Fig. 5 could represent either

(a) Albite twinning with $\perp(010)$ as twinning axis; composition An_{86}; or (b) Manebach twinning with $\perp(001)$ as twinning axis; composition An_{72}. The former is more likely if the twin is of the lamellar type. Further measurement gives

$$\perp^2CP_1 \wedge X_1 = 55^\circ$$
$$\wedge Y_1 = 67^\circ$$

The corresponding point *S* in Fig. 5, taken in conjunction with the previous alternative, confirms alternative (a).

Ambiguity is possible in some cases even after additional measurements have been made. Suppose, for example, that in the instance just described the point given by the second set of measurements were $T(\perp^2CP_1 \wedge X = 65^\circ;\ \perp^2CP_1 \wedge Y = 60^\circ)$. There are still two alternatives, of which the first is more likely to be the correct solution:

(a) Albite twinning, with transverse ($^2CP_1$) pericline lamellae; composition An_{86}.

(b) Manebach twinning, with transverse ($^2CP_1$) albite lamellae; composition An_{72}. Measurement of a Carlsbad twin in the same crystal removes all doubt.

(2) The curve for albite twinning—$\perp(010)$ in Fig. 5—is ambiguous over the range An_0 to An_{40}. That for $\perp(001)$ in Fig. 5 is also liable to ambiguity over the same range, if the plotted point falls inside and some distance from the ideal curve. Doubt is usually removed by plotting data for other subindividuals in the same crystal.

Example:

$\perp(010) \wedge X\ 90°$ } G in Fig. 5;
$\perp(010) \wedge Y\ 78°$ } An_9 or An_{32}.
In the same crystal $\perp(001) \wedge X\ 88°$ } H in Fig. 5;
$\perp(001) \wedge Y\ 18°$ } An_{33}.

The composition must be $An_{32}\pm$.

Axial angle and refractive index may also be used to solve certain cases, e.g. to distinguish An_{10} ($2V = 82°$, sign $+$; $\beta < \mu$ Canada balsam) from An_{32} ($2V = 83°$, sign $-$; $\alpha > \mu$ Canada balsam).

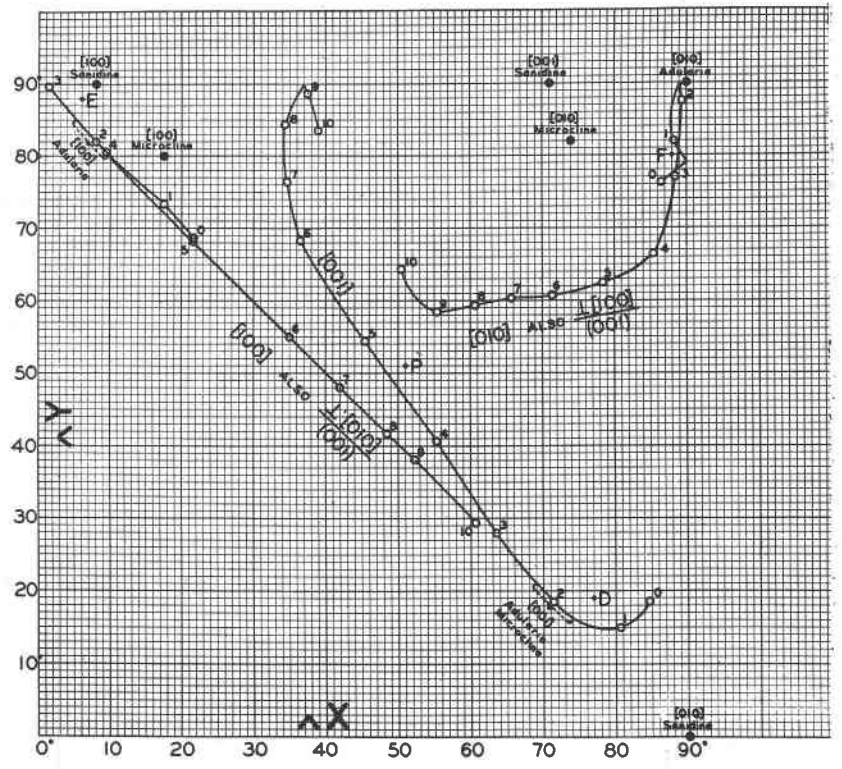

FIG. 6. Angles between X and Y and twinning axes of parallel and complex twins in plagioclase. Numbers 0–10 on each curve indicate anorthite contents 0–100%.

(b) *Ambiguous identity of the twinning axis in parallel and complex twins*

(1) It is impossible to distinguish optically between the twinning axes [100] and $\perp$[010]/(001), or again between [010] and $\perp$[100]/(001). In neither case would such a distinction have any practical importance, since the two axes of each pair are mutually inclined at very small angles. Each pair is therefore represented (within limits of experimental error) by a single curve in Fig. 6.

(2) When Z$\wedge \perp$CP (the pole of the main composition plane) is less than about 20°—i.e. when CP=(010) and the composition of the plagioclase is between An_0 and An_{40}—ambiguity arises if the second (transverse) set of planes measured in one of the main subindividuals is a set of twin lamellae. These are most likely to be pericline lamellae, the position of which in relation to the axes of the crystal lattice changes rapidly with variation in anorthite content in the more sodic plagioclases. This accounts for the irregular form of the broken curve of Fig. 4. Identification of the twinning axis is ambiguous in the case of points falling near *D*, *E*, *F*, *G* or *H* in Fig. 4. Nor is this ambiguity removed when appropriate data for X and Y are plotted alternatively on Figs. 6 and 7; for the very twinning axes that are liable to be confused in Fig. 4 have curves that lie close together in Figs. 6 and 7.

Example:

$$Z \wedge \perp CP_{1-2} = 8°$$
$$A_{1-2} \wedge \perp {}^2CP_1 = 15°$$

Plotted on Fig. 4, these figs. give a point close to *D*. Alternative interpretations.

(a) $A_{1-2}=[001]$; composition $=An_{15}\pm$.

(b) $A_{1-2}=\frac{\perp[100]}{(010)}$; composition $An_{15}\pm$.

Additional data from the same crystal are:

$$A_{1-2} \wedge X = 77°$$
$$A_{1-2} \wedge Y = 19°$$

Alternative interpretations:

(a) Figure 6, point *D*.
$A_{1-2}=[001]$; composition $=An_{15}$.

(b) Figure 7, point *D*.
$A_{1-2}=\frac{\perp[100]}{(010)}$; composition $=An_{13}$.

Although the composition has been determined as An_{13-15}, the identity of the twinning axis still remains uncertain. The only sure way to avoid ambiguity where plagioclase is a sodic variety, is to measure and plot a second set of cleavage planes ($^2Cl_1$ or $^2Cl_2$) instead of twin lamellae.

(3) Where the anorthite content of plagioclase is high (i.e. Z$\wedge \perp CP_{1-2}$ $=39°$–$47°$) the case in which $A_{1-2}\wedge \perp {}^2CP_{1-2}=5°\pm$ is insolubly ambiguous. Thus points in the vicinity of *A* in Fig. 4 are open to any of the following alternative interpretations:

(i) $CP_{1-2}=(010)$, $A_{1-2}=\frac{\perp[100]}{(010)}$; albite—ala twin.

(ii) $CP_{1-2}=(001)$, $A_{1-2}=[010]$; acline twin.

(iii) $CP_{1-2}=(001)$, $A_{1-2}=\frac{\perp[100]}{(001)}$; Manebach—ala twin, indistinguishable from acline twin by optical means.

(iv) CP_{1-2}=rhombic section, $A_{1-2}=[010]$; pericline twin.

The same ambiguity holds if a cleavage $^2Cl_1$ is measured instead of twin lamellae $^2CP_1$.

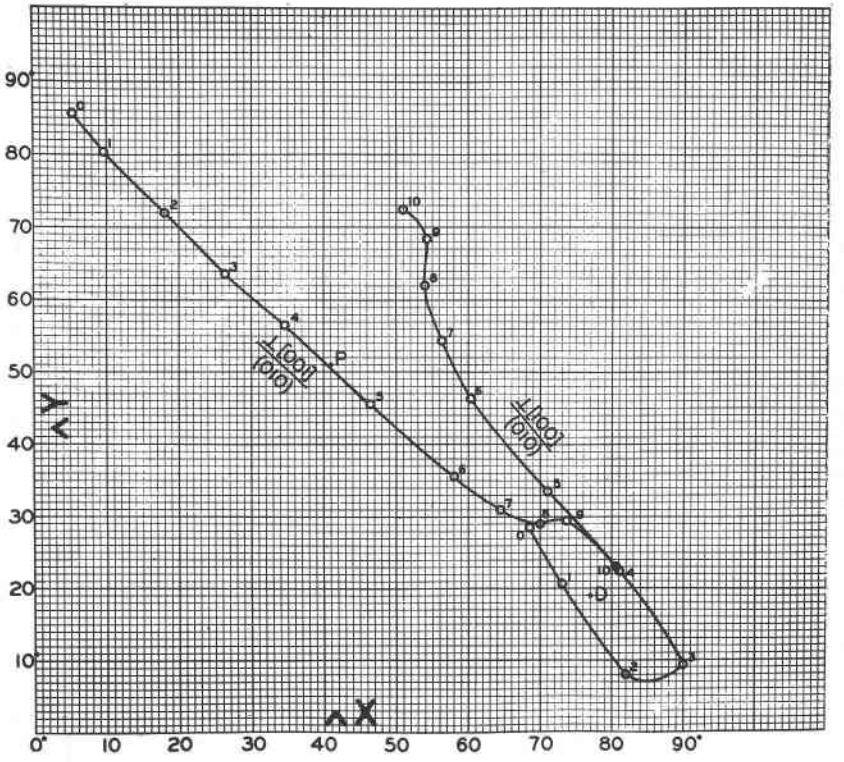

FIG. 7. Angles between X and Y and twinning axes of parallel and complex twins in plagioclase. Numbers 0–10 on each curve indicate anorthtite contents 0–100%.

(4) From Fig. 4 there would appear to be ambiguity for points in the vicinity of *B* and *C*. These correspond to calcic plagioclase with $Z/\backslash \perp CP_{1-2}=42°–47°$, in which the second set of measured lamellae ($^2CP_1$ or $^2CP_2$) proves to be due to pericline twinning. Such cases are solved when the angles $A_{1-2}/\backslash X$ and $A_{1-2}/\backslash Y$ are plotted on Figs. 6 and 7. The anorthite ends of the curves for [001] and $\perp[001]/(001)$ are sufficiently divergent over the range An_{80} to An_{100} to dispel any such ambiguity as may be apparent in the vicinity of *B* on Fig. 4.

(c) *Ambiguity as to composition in parallel and complex twins*

Any point falling on the curves for [100] or [010] or $\perp$ [100]/(010) in Figs. 6 and 7, within the range An_0 to about An_{40} is ambiguous with regard to anorthite content of the grain in question. The difficulty may usually be overcome by plotting data for other subindividuals of the same crystal.

Example:

$$\left.\begin{array}{l}[100] \wedge X = 6° \\ [100] \wedge Y = 88°\end{array}\right\} E \text{ in Fig. 6; } An_{26} \text{ or } An_{33}$$

In the same crystal

$$\left.\begin{array}{l}[010] \wedge X = 88° \\ [010] \wedge Y = 80°\end{array}\right\} F \text{ in Fig. 6; } An_{27} \text{ or } An_{3}$$

Composition must be $An_{26}\pm$.

General recommendations for avoiding ambiguity

The following recommendations are made with a view to obtaining results free of all ambiguity:

(1) When working with calcic plagioclase, An_{75} to An_{100}, use as far as possible parallel or complex twins with any of the following as twinning axes:

[001]; Carlsbad twin; Fig. 6.

$\frac{\perp[001]}{(010)}$; Carlsbad-albite twin; Fig. 7.

[100] or $\frac{\perp[010]}{(001)}$; Ala or Manebach-acline twin respectively; Fig. 6.

(2) For plagioclase of medium composition, An_{40} to An_{75}, any kind of twinning may be used without ambiguity.

(3) Determination of composition in sodic plagioclase, An_0 to An_{40}, is particularly liable to lead to ambiguous results. These may be avoided in three ways:

(a) Use twins where the composition plane $CP_{1-2}=(010)$; i.e. where $Z \wedge \perp CP_{1-2} < 20°$. Identify the twin axis A_{1-2} by measuring a second set of cleavages (e.g. $^2Cl_1$) rather than twin lamellae (e.g. $^2CP_1$). Use especially crystals showing Carlsbad twinning ($A_{1-2}=[001]$) or Carlsbad-albite twinning ($A_{1-2}=\perp[001]/(010)$).

(b) Use twins where the composition plane $CP_{1-2}=(001)$ or the rhombic section, i.e., where $Z \wedge \perp CP_{1-2} > 65°$. Measure fully at least three subindividuals so that points on two or three curves may be interpreted simultaneously.

(c) Highly sodic plagioclase An_0 to An_{10} can be distinguished from more calcic plagioclase An_{25} to An_{40} (with which it is liable to be con-

fused on curves for the common twins whose axes are ⊥(010) and [010]) by determining the optic axial angle and sign. For An_0 to An_{10} the sign is positive and the axial angle ranges from 71°–83°; for An_{25} to An_{40} the sign is negative and the axial angle 80°–90°.

Special Cases where X, Y or Z is Parallel to a Twinning Axis

If X is parallel to the twinning axis, then Y_1 coincides with Y_2 and Z_1 coincides with Z_2, and consequently there is no optical indication of twinning. A like condition holds good if either Y or Z is parallel to an axis of twinning. Inspection of the standard curves shows that this condition, although not precisely realized, is very closely approached in several instances of parallel and complex twinning in plagioclase:

(1) An_{17}; twinning axis [010]; $Z \wedge [010] = 1°$;

(2) An_{17}; twinning axis $\frac{\perp [100]}{(001)}$; $Z \wedge \frac{\perp [100]}{(001)} = 2°$.

(3) An_{30}; twinning axis [100]; $X \wedge [100] = 1\frac{1}{2}°$.

(4) An_{30}; twinning axis $\frac{\perp [010]}{(001)}$; $X \wedge \frac{\perp [010]}{(001)} = 1\frac{1}{2}°$.

Special Cases where X, Y or Z is Perpendicular to a Twinning Axis

Consider the special case where one of the three directions X, Y or Z is perpendicular to the twinning axis (e.g., Y in Fig. 10). Then this particular direction is the same in the two twinned subindividuals; and the other two pairs of directions, X_1, Z_1, X_2, Z_2 in Fig. 10, all lie in one plane, i.e., their poles lie on a single great circle of the projection. There may thus be a choice between two possible twinning axes—A and A′, the bisectors of the axis Z_1 Z_2 and X_1 X_2 in Fig. 10. Where, as in Fig. 10 the plane of X_1, Z_1, X_2 and Z_2 is oblique to the composition plane, graphic determination of the twinning axis still leads to a unique solution; since only one direction (in this case A) satisfies the second requirement of a twinning axis, viz., that it must lie normal to or within the composition plane.

There are three particular cases, however, where special conditions lead to solutions involving a choice of twinning axes, or to some other ambiguity. Each case is represented in the plagioclase series.

Case I Oligoclase, An_{22}, twinned with (010) *as composition plane.* The special condition for oligoclase, An_{22} is that Z is normal to the composition plane (010) (cf. Fig. 3), i.e., to any twinning axis lying within that plane. This leads to the following conditions peculiar to oligoclase of this particular composition:

(1) In any instance of parallel or complex twinning with (010) as composition plane graphic determination of the twinning axis leads to two alternative solutions. In the example shown in Fig. 8, twinning on either [001] (A) or $\perp[001]/(010)$ (A′) would account equally well for the relative orientation of the two subindividuals concerned. In other cases there is a similar choice between [100] and $\perp[100]/(010)$. If the data for X and Y are plotted on the two appropriate curves of Figs. 6 and 7, the compositions so determined are identical, as shown in the following example projected in Fig. 8:

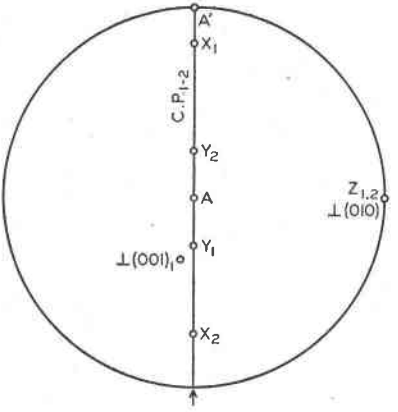

FIG. 8. Equal-area projection for oligoclase An_{22} twinned with [001]=A or $\frac{\perp[001]}{(010)}$=A′ as alternative twinning axes. C.P.=composition plane, (010).

$A \wedge \perp^2Cl_1 = 26°$; therefore A=[001]

$A' \wedge \perp^2Cl_1 = 64°$; therefore $A' = \frac{\perp[001]}{(010)}$

$\left.\begin{matrix} A \wedge X = 70° \\ A \wedge Y = 20° \end{matrix}\right\}$ From [001] curve, Fig. 6, composition = An_{22}.

$\left.\begin{matrix} A' \wedge X = 20° \\ A' \wedge Y = 70° \end{matrix}\right\}$ From $\frac{\perp[001]}{(010)}$ curve, Fig. 7, composition = An_{22}.

In actual practice a similar choice of twinning axes exists for oligoclase ranging from An_{20} to An_{25}; for Z_1 and Z_2 so nearly coincide that slight errors in location of either lead to great elongation of the triangle of error along the obliquely intersecting arcs X_1, X_2 and Y_1, Y_2.

(2) If two subindividuals of composition An_{22} are twinned on the albite law, i.e., by reflection across (010), their optic orientations are

identical; i.e., for this precise composition albite twinning cannot be detected optically.

(3) The optic orientation of oligoclase, An_{22} is almost identical with that of low-temperature orthoclase (adularia), such as occurs in plutonic and metamorphic rocks. When feldspar occurs in scattered untwinned grains, as in many metamorphic rocks, or in small simply twinned laths in the groundmass of lavas, oligoclase may readily be confused with orthoclase unless refractive index tests can be made.

A similar condition is closely approached in oligoclase, An_{17} to An_{20}, twinned on the pericline law. In this case Y makes an angle of 87°–89° with the rhombic section, cf. Fig. 5.

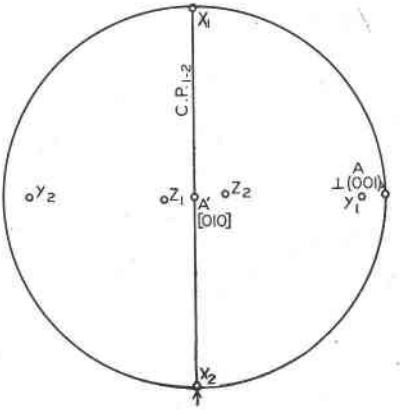

FIG. 9. Equal-area projection for oligoclase-andesine An_{30} twinned with ⊥(001) = A or [010] = A′ as alternative twinning axes. CP_{1-2} = composition plane (001).

Case II. Sodic plagioclase with X or Z normal to twinning axis and parallel to composition plane. If one of the directions X, Y or Z is normal to a twinning axis and also lies in the composition plane, graphic determination of the twinning axis again leads to two solutions. Here there is a choice between an axis of normal twinning, and one of parallel or complex twinning. Within limits of experimental error, this condition is fulfilled for plagioclase of various compositions within the range of oligoclase.

(a) Oligoclase-andesine, An_{30}; X lies in (001); X is almost normal to ⊥[100]/(001), which coincides with, and cannot be distinguished optically from [010]. Graphic determination of the twinning axis (Fig. 9) leads to two alternatives, either ⊥(001) (A), or [010] = ⊥[100]/(001) (A′).

(b) Oligoclase, An_{18}; Z lies in (001); Z is nearly normal to [100] = ⊥[010]/(001). Within the limits of experimental error there is a choice between ⊥(001), and [100] = ⊥[010]/(001) as twinning axes.

(c) Albite and oligoclase, An_3 to An_{30}; X is very nearly parallel to (010); X is very nearly perpendicular to [010].

Case III. Simulation of normal twinning (*Bytownite An_{85}*). An essential part of the Emmons procedure for determining feldspars with a five-axis stage, and a useful check in the zone method of Rittmann, is the direct microscopic distinction between normal twins and twins of the parallel or complex type (Emmons and Gates, 1939, p. 579; Emmons, 1943, pp. 104, 129). The composition plane of the twinned crystal is

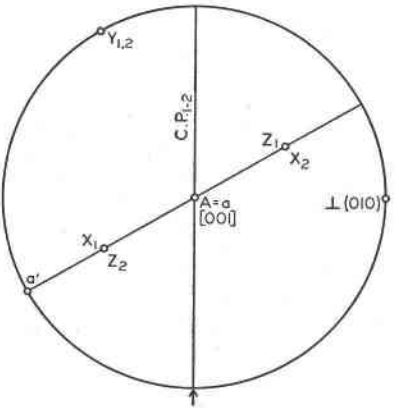

FIG. 10. Ideal case of Carlsbad twinning—[001]=twinning axis—to give coincidence of optic axes (a, a') in both subindividuals (cf. An_{85}).

brought parallel to the vertical N–S plane, and the crystal is now tilted through any angle about the E–W axis of the stage, i.e., about the normal to the composition plane. If the change in interference color is identical in the two subindividuals, i.e., if they remain exactly matched in color throughout tilting, the twin is diagnosed as a normal twin; if the color change is unequal, the twin is parallel or complex.

In his intensive study of feldspars in some Indian basalts, Barber (1936*a*, pp. 258–262) noted five separate instances where bytownite, An_{85}, twinned on the Carlsbad law gave the optical reaction of a normal twin, when treated as just described. He concluded that "in feldspars of this composition (85 per cent. An.) the birefringence of two hemitropes twinned according to the Carlsbad law is equal in all positions in the zone perpendicular to (010)" (Barber, 1936*a*, p. 262). No further explanation was offered. It was pointed out that this phenomenon had been observed only in bytownite (An_{85}) but that it nevertheless illustrates "the danger of relying on curtailed procedure for the recognition of the twinning law."

It would seem that the phenomenon recorded by Barber could occur in any feldspar in which the following three conditions, illustrated in projection in Fig. 10, were simultaneously fulfilled:

(a) Y is perpendicular to the twinning axis [001], A, but is inclined at any angle to the composition plane (010).

(b) $2V=90°$

(c) The twinning axis, [001], makes angles of 45° with X and Z respectively. Under these conditions (and in no other circumstances) both optic axes of the two twinned subindividuals coincide; one pair also coincides with twinning axis, A.

The interference color shown by any section of plagioclase depends upon the relative retardation of the emergent rays; and this, for a given thickness of section and a given angle of tilt on E–W, depends upon the angles between the emergent ray and each of the optic axes.* These same angles also determine the vibration directions of the emergent rays,† and so in turn the intensity of illumination of a section as seen between crossed nicols. Now, for any degree of tilt on E–W, the two subindividuals of the ideal twin of Fig. 10 have in common the two optic axes (a and a') and the direction of the emergent ray (which must lie in the composition plane). Consequently both subindividuals show exactly the same interference tint and equal intensity of illumination.

Bytownite, An_{85}, does not exactly conform to the ideal conditions depicted in Fig. 10: but it approximates sufficiently closely to account for the phenomenon recorded by Barber. The angle $Y \wedge [001]$, as indicated in Fig. 6, is 88°; 2 V, according to data recorded by Barber (1936*a*, p. 277) is close to 85°; the angles $X \wedge [001]$ and $Z \wedge [001]$, measured from Barber's (1936*a*, p. 261) stereographic projection are 35° and 55°, respectively. This appears to be the only case in the plagioclase series, in which all three conditions specified above approach fulfillment.

There are two additional general cases, however, in which it may be difficult or impossible to distinguish between normal and parallel twins by the optical means described by Emmons:

(a) If X or Y or Z is normal to the composition plane, then both subindividuals remain in extinction when the crystal is rotated about the normal after the latter has been brought to coincide with the E–W axis of the stage. This is true for oligoclase An_{22} twinned on any law with (010) as composition plane; and it is very nearly true for oligoclase, An_{17} to An_{20}, twinned on the pericline law.

* Johannsen (1918, pp. 351–355) derives the equation

$$\gamma' - \alpha' = (\gamma - \alpha) \sin \theta \sin \theta'$$

where $\gamma' - \alpha'$ = relative retardation of a random section, and θ and θ' are respective angles between the emergent ray (the normal to the section) and the two optic axes.

† The vibration directions bisect the angles of intersection of the traces of the two planes each of which contains the direction of the emergent ray and one optic axis.

(b) Where X, Y or Z is nearly parallel to a twinning axis for medium and calcic oligoclase, the optic axes of one subindividual very nearly coincide with those of the other. The optical behavior of the two subindividuals should therefore be almost identical when the crystal is rotated about the normal to the composition plane.

Determinations on Zoned Crystals and Microlites

When plagioclase crystals are strongly zoned, where adjoining lamellae are notably different in composition, or when the crystals to be measured are small laths or microlites in which X, Y and Z can be measured in only one subindividual, it is obviously impossible or undesirable to use a twinning axis as the crystallographic direction of reference with which to compare the positions of X, Y, and Z in the lattice. In such cases a cleavage or composition plane is measured as accurately as possible and its pole plotted directly on the projection and used as the reference point. The directions X, Y and Z are measured in such lamellae and zones as are large enough for this, and plotted on the projection. Appropriate angles can now be measured and the anorthite content determined from the curves of Fig. 5.

This method, though quick, is somewhat inaccurate. It is difficult to locate cleavage or composition planes precisely by microscopic means, especially if they are inclined at less than 75° to the plane of the section. Composition planes are usually more sharply defined and more continuous than cleavage planes; but they are liable to be determined by vicinal faces (cf. Barber, 1936*a*, pp. 233, 236), whereas cleavage faces must always be rational.

An alternative method is that of Rittmann (1929) generally referred to as the "zone method." This has been described fully by various writers (e.g. Barber, 1936*a*, pp. 278–281; Emmons, 1943, pp. 115–134) and need not be considered further here, beyond noting that some experienced workers (e.g. Barber, 1936*a*, p. 281) consider it unsatisfactory and inaccurate. It is, however, the only practicable method for determining composition of very narrow zones of microlites (usually elongated parallel to *a*) so small that X, Y, and Z cannot be located accurately.

Departures from Standard Curves

A number of writers have commented upon the commonly observed discrepancy between points plotted from data measured by the universal stage, and the ideal curves given by Duparc and Reinhard (1924), Nikitin (1936) and others. The same applies to the equivalent curves of Figs. 5, 6 and 7.

The most comprehensive discussion of this topic in English, illustrated

by abundant experimental data, is that of Barber (1936*a*, pp. 230–258) who concluded that the physical conditions, especially temperature, prevailing at the time of crystallization are probably responsible for the observed variation. Barber dismissed variation in potash content, as having minor influence only, and discounted inaccuracies in measurement, inaccuracies in the standard curves, and errors due to vicinal faces as composition planes, as possible causes of the discrepancies noted. The problem is still not satisfactorily solved. In a subsequent paper Barber (1936*b*) recorded some experimental results which failed to confirm his hypothesis of temperature control; but several European workers, notably Köhler (1942*a*, 1942*b*), Scholler (1942), Tertsch (1942), and Oftedahl (1944) have since brought forward additional experimental evidence pointing to the existence of appreciable optical differences between high- and low-temperature plagioclases of corresponding compositions. The latest account, accompanied by a full list of European references, is that of E. Wenk (1945, pp. 368–371).

The writer records his own experience that optical data for andesine and labradorite in basic and semibasic lavas and sills in eastern Otago, New Zealand, consistently depart appreciably, sometimes by as much as 10°, from the standard curves (cf. Benson and Turner, 1940, pp. 196, 198; Benson, 1944, pp. 74, 75). This might well be attributed to the high temperatures and low pressures typical of volcanic conditions; but there is also the possibility of a chemical influence, for many of the rocks in question are notably alkaline.

Acknowledgments

The writer wishes to acknowledge his gratitude to Mr. Theo. H. Crook who very kindly prepared all diagrams accompanying this paper. His thanks are also due to Professor A. Pabst for helpful discussion on a number of points relating to optics of twinned plagioclase.

References

Barber, C. T. (1936*a*), The Tertiary igneous rocks of the Pakokku District and the Salingyi Township of the Lower Chindwin District, Burma, with special reference to the determination of the feldspars by the Fedoroff Method: *Mem., Geol. Sur. India*, **68**, pt. 2.

——— (1936*b*), The effect of heat on the optical orientation of plagioclase feldspars: *Mineral. Mag.*, **24**, 343–352.

Benson, W. N. (1944), The basic igneous rocks of Eastern Otago and their tectonic environment, Part IV: *Trans. Roy. Soc. New Zealand*, **74**, pt. 1, 71–123.

——— and Turner, F. J. (1940), Mugearites in the Dunedin district: *Trans. Roy. Soc. New Zealand*, **70**, pt. 3, 188–199.

Duparc, L., and Reinhard, M. (1924), La Détermination des Plagioclases dans les Coupes Minces: *Mem. Soc. Phys. and Hist. Nat. Genève*, **40**, fasc. 1.

EMMONS, R. C. (1943), The Universal Stage: *Mem. Geol. Soc. Am.*, no. **8.**

———, AND GATES, R. M. (1939), New method for the determination of feldspar twins: *Am. Mineral.*, **24,** 577–589.

JOHANNSEN, A. (1918), *Manual of Petrographic Methods*, McGraw-Hill, New York.

KÖHLER, A. (1942a), Die Abhängigkeit der Plagioklasoptik von vergangenen Wärmeverhalten: *Min. Petr. Mitt.*, **53,** 24–49.

——— (1942*b*), Drehtischmessungen an Plagioklaszwillingen von Tief- und Hochtemperaturoptik: *Min. Petr. Mitt.*, **53,** 159–179

NIKITIN, W. (1936), *Die Fedorow-Methode*, Borntraeger, Berlin.

OFTEDAHL, C. (1944), High temperature optics in plagioclases of the Oslo region: *Norsk Geol. Tidssk.*, **24,** 75–78.

SCHOLLER, H. (1942), Versuche zur Temperaturabhängigkeit der Plagioklasoptik: *Min. Petr. Mitt.*, **53,** 180–221.

TERTSCH, H. (1942), Zur Hochtemperaturoptik basischer Plagioklase: *Min. Petr. Mitt.*, **54,** 193–217.

WENK, E. (1945), Kritischer Vergleich von Anorthitbestimmungen an Plagioklasen: *Schweiz. Min. Petr. Mitt.*, **25,** 349–382.